research papers

Packing effects on the geometry of neutral platinum(II) complexes due to solvate molecules: the structure of *trans*-dichlorobis(triphenylarsine)-platinum(II)

Maria H. Johansson,[a]* Stefanus Otto,[b] Andreas Roodt[b] and Åke Oskarsson[a]

[a]Inorganic Chemistry 1, Centre for Chemistry and Chemical Engineering, University of Lund, PO Box 124, S-221 00 Lund, Sweden, and [b]University of the Orange Free State, PO Box 339, Bloemfontein 9300, South Africa

Correspondence e-mail:
maria.johansson@inorg.lu.se

A series of structures of *trans*-dichlorobis(triphenylarsine)-platinum(II), recrystallized from four different solvents, have been characterized by X-ray crystallography and were shown to crystallize as different solvates (same metal complex, different crystallization solvents). Their geometric differences induced by packing and solvent molecules were analysed with half-normal probability plots and root-mean-square deviations. The recrystallization solvents used in the investigation were 1,1,1-trichloroethane, dichloromethane, 1,2-dichloroethane and benzene, and the following crystallization modes were obtained. From 1,1,1-trichloroethane the metal complex crystallizes without solvent as *trans*-$[PtCl_2(AsPh_3)_2]$ in $P2_1/n$ with $Z = 2$, $a = 9.271\ (2)$, $b = 19.726\ (4)$, $c = 9.830\ (2)$ Å, $\beta = 111.83\ (3)°$, $V = 1668.8\ (6)$ Å^3, $R = 0.0262$, and from dichloromethane with two solvent molecules as *trans*-$[PtCl_2(AsPh_3)_2]\cdot2CH_2Cl_2$ in $Pbca$ with $Z = 4$, $a = 20.582\ (4)$, $b = 8.146\ (2)$, $c = 23.491\ (5)$ Å, $V = 3938.5\ (14)$ Å^3 and $R = 0.0316$. From dichloroethane it crystallizes with one solvent molecule as *trans*-$[PtCl_2$-$(AsPh_3)_2]\cdot C_2H_4Cl_2$ in $P\bar{1}$ with $Z = 1$, $a = 9.390\ (2)$, $b = 9.548\ (2)$, $c = 11.931\ (2)$ Å, $\alpha = 109.70\ (3)$, $\beta = 108.26\ (3)$, $\gamma = 98.77\ (3)°$, $V = 915.6\ (3)$ Å^3, $R = 0.0390$, and from benzene with half a solvent molecule as *trans*-$[PtCl_2(AsPh_3)_2]\cdot$-$0.5C_6H_6$ in $P2_1/n$ with $Z = 4$, $a = 11.778\ (2)$, $b = 18.712\ (4)$, $c = 16.647\ (3)$ Å, $\beta = 104.78\ (3)°$, $V = 3547.3\ (12)$ Å^3 and $R = 0.0303$. In all four compounds platinum(II) coordinates to triphenylarsine and chloride in a pseudo-square-planar *trans* configuration. The Pt—As distances are in the range 2.4104 (4)–2.3923 (4) Å and the Pt—Cl distances are in the range 2.309 (2)–2.2839 (9) Å. The solvents have a large influence on the packing, resulting in different space groups or different occupancies in the same space group. Half-normal probability plots show that the largest geometric differences, within the metal complex, are in the bond and torsion angles around the As—C bonds. Very similar torsion angles were observed around the Pt—As bond for all the structures, except for one AsPh$_3$ ligand in the benzene solvate, which differs by about 10° from the others. The metal–donor bond distance varies by as much as 0.019 and 0.025 Å (95% confidence interval) for Pt—As and Pt—Cl, respectively. The variations are essentially caused by intermolecular interactions. Packing efficiency is expressed as the volume filled by each metal complex in the unit cell and is calculated by subtracting the sum of the solvent molecule volumes from the total volume of the unit cell and then dividing by Z. The efficiency is largest in the dichloroethane solvate and smallest in the non-solvated compound, with a difference of approximately 22 Å^3 per metal complex.

1. Introduction

The observed geometry of a metal complex in the solid state is often discussed in terms of intramolecular forces alone, thus neglecting packing effects (Belsky *et al.*, 1990). The influence of environment on shape and dimensions can be investigated by studying a particular metal complex in different crystallographic environments. This can be achieved in a number of ways, *i.e.* the study of crystal structures with more than one molecule in the asymmetric unit (Lövqvist, 1996), of polymorphs (Kapoor *et al.*, 1996), the study of structures with different counter ions (charged complex; Ericson *et al.*, 1992) or of different crystalline solvates of a complex. Several examples in the literature are described where solvents were shown to have a great influence on the crystallization mode of a specific complex. A well known example is *trans*-[Rh(CO)(Cl)(PPh₃)₂] for which several polymorphs and different solvates are reported (Kemp *et al.*, 1995). During the initial preparation of the extensively studied *trans*-[PtHCl(PPh₃)₂] complex, some difficulties were encountered, which were later shown to be induced by isolation from different solvent media (Collimati *et al.*, 1970).

It may be convenient to divide metal complexes into two groups, *i.e.* neutral and charged complexes, since the geometry of the latter may be modulated by a fairly strong electric field originating from the distribution of cations and anions in the structure.

This paper is devoted to describing the geometry of the neutral complex *trans*-[PtCl₂(AsPh₃)₂], as observed in four different crystallographic environments. This Pt^{II} complex was prepared in a systematic study of syntheses and reactivity of bis-tertiary arsine complexes (Watkins, 1970; Roodt *et al.*, 1995; Otto & Roodt, 1996, 1997). The structures of the four compounds, *i.e.* the pure complex and three solvates as determined by single-crystal X-ray crystallography, are discussed in terms of their packing efficiency (Kitaigorodsky, 1973). Differences in geometry of the metal complex in the

different compounds are analysed by root-mean-square (RMS) calculations and half-normal probability plots (De Camp, 1973; Abrahams & Keve, 1971).

2. Experimental

2.1. Synthesis

The title complex was prepared by the addition of an excess of AsPh₃ (1.796 mmol, 550 mg) to an acetone solution (20 ml) of *cis*- and *trans*-[PtCl₂(SMe₂)₂] (0.513 mmol, 200 mg; Cox *et al.*, 1934). The desired product precipitates spontaneously in near quantitative yield as predominantly the *trans* isomer, and was recrystallized from 1,1,1-trichloroethane, dichloromethane, 1,2-dichloroethane and benzene to give *trans*-[PtCl₂(AsPh₃)₂], (1), *trans*-[PtCl₂(AsPh₃)₂]·2CH₂Cl₂, (2), *trans*-[PtCl₂(AsPh₃)₂]·C₂H₄Cl₂, (3), and *trans*-[PtCl₂-(AsPh₃)₂]·0.5C₆H₆, (4).

2.2. Crystallography and calculations

The crystal data and details of the data collection and refinement are given in Table 1.[1] In all structures the first 50 frames were collected again at the end to check for decay. No decays were observed. All reflections were merged and integrated using *SAINT* (Siemens, 1995). Corrections were applied for Lorentz and polarization effects as well as absorption using multi-scans (Sheldrick, 1996).

All non-H atoms were refined with anisotropic displacement parameters, while the H atoms were constrained to parent sites, using a riding model. For (3), residual electron density peaks of 1.04 and −2.01 were encountered within 1.2 Å of the platinum centre, while no high residues (>1.0) were found in any of the other structures. All structures were checked for solvent accessible cavities using *PLATON* (Spek, 1990) and the graphics were performed with *DIAMOND* (Brandenburg, 1997). The RMS calculations were performed with *SHELXL*97 (Sheldrick, 1997) and the half-normal probability plots with *EXCEL*97 (Microsoft, 1997).

3. Results and discussion

3.1. Description of the structures

A numbering scheme for (1) is given in Fig. 1 and the other complexes were numbered accordingly. Packing diagrams for (1), (2), (3) and (4) are shown in Fig. 2. The title complex has a distorted square-planar coordination around platinum with the triphenylarsine ligands in *trans* positions to each other. In (1), (2) and (3) the Pt atom is situated on special positions (inversion centres).

In (1) (Fig. 2*a*) one of the phenyl rings is orientated along the *Z*-axis and all the molecules are stacked on top of each other in both the *X*- and *Z*-directions.
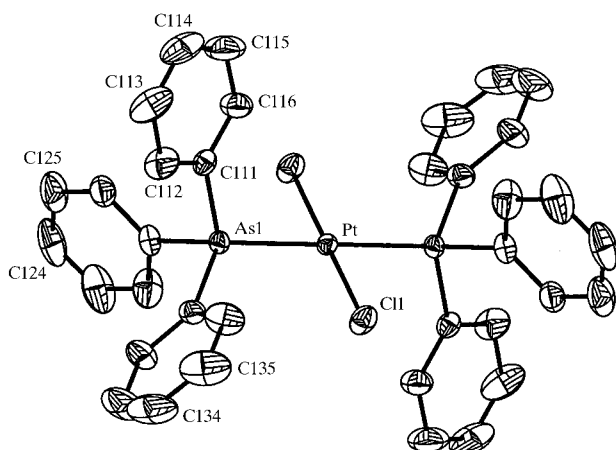
Figure 1
The numbering scheme for *trans*-dichlorobis(triphenylarsine)platinum(II) showing the thermal ellipsoids of (1) (30% probability). H atoms are omitted for clarity. The other complexes are numbered accordingly, with the first digit referring to the number of the ligand, the second to the ring and the third to the C atoms.

Table 1
Experimental details.

	(1)	(2)	(3)	(4)
Crystal data				
Chemical formula	$PtCl_2[As(C_6H_5)_3]_2$	$PtCl_2[As(C_6H_5)_3]_2\cdot 2CH_2Cl_2$	$PtCl_2[As(C_6H_5)_3]_2\cdot C_2H_4Cl_2$	$PtCl_2[As(C_6H_5)_3]_2\cdot 1/2C_6H_6$
Chemical formula weight	878.43	1048.28	977.38	917.48
Cell setting	Monoclinic	Orthorhombic	Triclinic	Monoclinic
Space group	$P2_1/n$	$Pbca$	$P\bar{1}$	$P2_1/n$
a (Å)	9.2706 (19)	20.582 (4)	9.3899 (19)	11.778 (2)
b (Å)	19.726 (4)	8.1460 (16)	9.5481 (19)	18.712 (4)
c (Å)	9.830 (2)	23.491 (5)	11.931 (2)	16.647 (3)
α (°)	90	90	109.70 (3)	90
β (°)	111.83 (3)	90	108.26 (3)	104.78 (3)
γ (°)	90	90	98.77 (3)	90
V (Å^3)	1668.8 (6)	3938.5 (14)	915.6 (3)	3547.3 (12)
Z	2	4	1	4
D_x (Mg m^{-3})	1.748	1.768	1.773	1.718
Radiation type	Mo $K\alpha$	Mo $K\alpha$	Mo $K\alpha$	Mo $K\alpha$
Wavelength (Å)	0.71073	0.71073	0.71073	0.71073
No. of reflections for cell parameters	8192	8192	4985	8150
θ range (°)	2–30	2–30	2–30	2–30
μ (mm^{-1})	6.355	5.664	5.942	5.984
$F(000)$	848	2032	474	1780
Temperature (K)	293 (2)	293 (2)	293 (2)	293 (2)
Crystal form	Cube	Rectangle	Needle	Cube
Crystal size (mm)	$0.20 \times 0.19 \times 0.17$	$0.49 \times 0.24 \times 0.23$	$0.20 \times 0.08 \times 0.07$	$0.27 \times 0.27 \times 0.25$
Crystal colour	Yellow	Yellow	Yellow	Yellow
Data collection				
Diffractometer	SMART CCD	SMART CCD	SMART CCD	SMART CCD
Data collection method	ω scans	ω scans	ω scans	ω scans
Absorption correction	Multi-scan	Multi-scan	Multi-scan	Multi-scan
T_{min}	0.295	0.172	0.341	0.295
T_{max}	0.366	0.280	0.584	0.316
No. of measured reflections	13 750	35 863	7759	29 416
No. of independent reflections	5096	7901	5381	10 893
No. of observed reflections	4229	5609	4450	8597
Criterion for observed reflections	$I > 2\sigma(I)$	$I > 2\sigma(I)$	$I > 2\sigma(I)$	$I > 2\sigma(I)$
R_{int}	0.0286	0.0264	0.0278	0.0309
θ_{max} (°)	31.60	34.34	31.65	31.70
Range of h, k, l	$-13 \rightarrow h \rightarrow 8$ $-27 \rightarrow k \rightarrow 28$ $-13 \rightarrow l \rightarrow 14$	$-29 \rightarrow h \rightarrow 32$ $-8 \rightarrow k \rightarrow 12$ $-34 \rightarrow l \rightarrow 36$	$-13 \rightarrow h \rightarrow 10$ $-13 \rightarrow k \rightarrow 11$ $-13 \rightarrow l \rightarrow 17$	$-16 \rightarrow h \rightarrow 17$ $-27 \rightarrow k \rightarrow 20$ $-24 \rightarrow l \rightarrow 22$
Refinement				
Refinement on	F^2	F^2	F^2	F^2
$R[F^2 > 2\sigma(F^2)]$	0.0262	0.0316	0.0390	0.0303
$wR(F^2)$	0.0608	0.0670	0.0976	0.0652
S	1.048	1.201	0.916	1.061
No. of reflections used in refinement	5096	7901	5381	10 893
No. of parameters used	190	214	205	397
H-atom treatment	Riding model	Riding model	Riding model	Riding model
Weighting scheme	$w = 1/[\sigma^2(F_o^2) + (0.0247P)^2 + 0.5297P]$ where $P = (F_o^2 + 2F_c^2)/3$	$w = 1/[\sigma^2(F_o^2) + (0.0164P)^2 + 3.4151P]$ where $P = (F_o^2 + 2F_c^2)/3$	$w = 1/[\sigma^2(F_o^2) + (0.0557P)^2]$ where $P = (F_o^2 + 2F_c^2)/3$	$w = 1/[\sigma^2(F_o^2) + (0.0207P)^2 + 1.6655P]$ where $P = (F_o^2 + 2F_c^2)/3$
$(\Delta/\sigma)_{max}$	0.029	0.001	0.001	0.004
$\Delta\rho_{max}$ (e Å^{-3})	0.973	0.853	1.039	0.711
$\Delta\rho_{min}$ (e Å^{-3})	-0.997	-0.742	-2.011	-0.982
Source of atomic scattering factors	*International Tables for Crystallography* (1992, Vol. C, Tables 4.2.6.8 and 6.1.1.4)	*International Tables for Crystallography* (1992, Vol. C, Tables 4.2.6.8 and 6.1.1.4)	*International Tables for Crystallography* (1992, Vol. C, Tables 4.2.6.8 and 6.1.1.4)	*International Tables for Crystallography* (1992, Vol. C, Tables 4.2.6.8 and 6.1.1.4)
Computer programs				
Data collection	*SMART* (Siemens, 1996)	*SMART* (Siemens, 1996)	*SMART* (Siemens, 1996)	*SMART* (Siemens, 1996)
Cell refinement	*SAINT* (Siemens, 1995)	*SAINT* (Siemens, 1995)	*SAINT* (Siemens, 1995)	*SAINT* (Siemens, 1995)

Table 1 (continued)

	(1)	(2)	(3)	(4)
Data reduction	SHELXTL97 (Sheldrick, 1997b)	SHELXTL97 (Sheldrick, 1997b)	SHELXTL97 (Sheldrick, 1997b)	SHELXTL97 (Sheldrick, 1997b)
Structure solution	SHELXS86 (Sheldrick, 1990)	SHELXS86 (Sheldrick, 1990)	SHELXS86 (Sheldrick, 1990)	SHELXS86 (Sheldrick, 1990)
Structure refinement	SHELXL97 (Sheldrick, 1997a)	SHELXL97 (Sheldrick, 1997a)	SHELXL97 (Sheldrick, 1997a)	SHELXL97 (Sheldrick, 1997a)
Preparation of material for publication	SHELXTL97 (Sheldrick, 1997b)	SHELXTL97 (Sheldrick, 1997b)	SHELXTL97 (Sheldrick, 1997b)	SHELXTL97 (Sheldrick, 1997b)

In (2) (Fig. 2b) the platinum molecules are tilted alternatively relative to the X-axis. The solvent molecules are stacked in the space between two metal complexes which are tilted away from each other and are related via an inversion centre. The two H atoms in CH_2Cl_2 point towards the chloride in the nearest platinum complex, with the closest $Cl\cdots H$ contact being 2.74 Å.

Complex (3) (Fig. 2c) has the Pt—As bonds along the c-axis. Both the platinum and the solvent molecule lie on inversion centres [(0, 0, 0) and $(\frac{1}{2}, 0, \frac{1}{2})$, respectively] in $P\bar{1}$ giving $Z = 1$. The solvent molecule is affected by disorder, resulting in an unrealistic geometry. The H atoms in dichloroethane are directed towards the chlorides in the metal complex, with the closest $Cl\cdots H$ contact being 3.05 Å.

In (4) (Fig. 2d) the Cl—Pt—Cl and As—Pt—As bonds are almost parallel to the b- and a-axes, respectively. In this compound only the benzene solvent molecules are situated on special positions and they are stacked in chains in the middle of the cell and along the a-axis. The closest contact from chloride to a benzene H atom is 3.23 Å.

The volumes of the solvent molecules have been estimated from their crystal structures to be 132 Å^3 (trichloroethane; Silver & Rudman, 1972), 82 Å^3 (dichloromethane; Kawaguchi et al., 1973), 103 Å^3 (1,2-dichloroethane; Boese et al., 1992) and 123 Å^3 (benzene; Bacon et al., 1964). Assuming that the packing of these solvents is equally efficient, the calculated volumes can be used to measure which of the complexes reported here has the most efficient packing. By subtracting the sum of the volumes of the solvent molecules in the unit cell from the volume of the unit cell and dividing by Z, the volume of the Pt complex can be obtained. The volumes of the complexes were calculated as 821, 813 and 824 Å^3 for (2), (3) and (4), respectively, compared with 834 Å^3 for (1), which contains no solvent molecule. The largest solvent molecule, trichloroethane, seems to be unable to fit into any acceptable packing arrangement. The Pt complex thus packs most efficient with 1,2-dichloroethane as solvent (3), while dichloromethane (2) and benzene (4) are intermediate and the structure
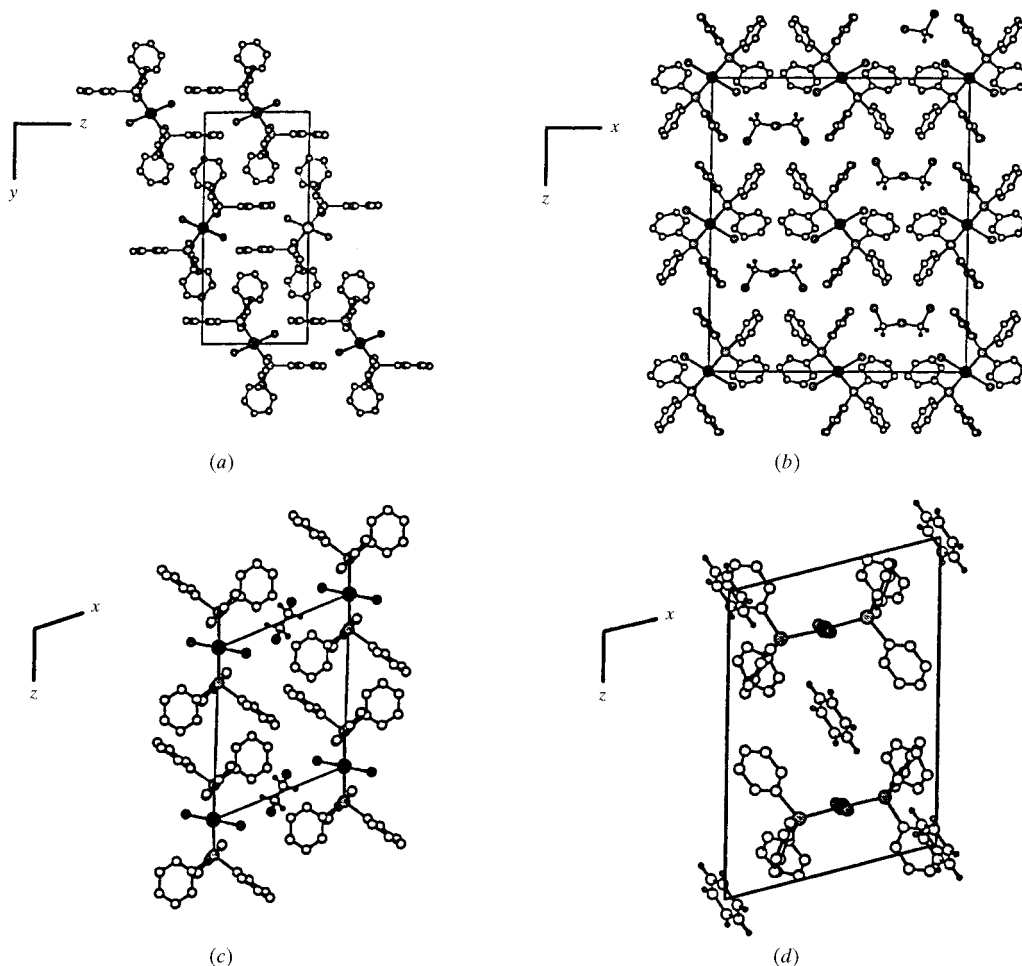

Figure 2
Packing diagrams of (a) (1), (b) (2), (c) (3) and (d) (4).

Table 2
Selected bond distances (Å), bond angles (°) and torsion angles (°) in (1), (2), (3) and (4).

	(1)	(2)	(3)	(4a)	(4b)
Pt—Cl	2.3003 (11)	2.3006 (8)	2.3086 (17)	2.2975 (9)	2.2839 (9)
Pt—As	2.4104 (4)	2.3923 (4)	2.4068 (6)	2.4092 (6)	2.4063 (6)
As—C111	1.938 (3)	1.938 (3)	1.929 (4)	1.938 (3)	1.938 (3)
As—C121	1.933 (3)	1.930 (3)	1.936 (4)	1.934 (3)	1.935 (3)
As—C131	1.939 (3)	1.938 (3)	1.952 (5)	1.935 (3)	1.946 (3)
Cl1—Pt—Cl1′	180	180	180	178.79 (3)	
Cl1—Pt—As1′	88.33 (3)	86.98 (2)	88.31 (5)	88.50 (2)	
Cl1′—Pt—As1′	91.67 (3)	93.02 (2)	91.69 (5)	91.62 (2)	
Cl1—Pt—As1	91.67 (3)	93.02 (2)	91.69 (5)	93.20 (2)	
Cl1′—Pt—As1	88.33 (3)	86.98 (2)	88.31 (5)	86.62 (2)	
As1′—Pt—As1	180	180	180	176.692 (11)	
Pt—As1—C111	112.94 (9)	112.55 (8)	112.02 (14)	110.11 (10)	113.66 (9)
Pt—As1—C121	112.43 (9)	111.72 (8)	112.99 (14)	114.68 (9)	111.53 (9)
Pt—As1—C131	119.79 (10)	119.73 (8)	119.83 (13)	121.26 (9)	117.53 (9)
C111—As1—C121	103.59 (13)	106.74 (11)	106.5 (2)	103.44 (13)	104.43 (13)
C111—As1—C131	102.50 (13)	101.99 (12)	102.0 (2)	103.57 (12)	103.96 (13)
C121—As1—C131	103.85 (15)	102.82 (12)	102.1 (2)	101.85 (12)	104.48 (14)
Cl1—Pt—As1—C111	104.22 (10)	107.13 (8)	104.22 (15)	95.17 (10)	103.88 (10)
Cl1—Pt—As1—C121	−138.98 (12)	−132.80 (9)	−135.50 (15)	−148.69 (10)	−138.39 (11)
Cl1—Pt—As1—C131	−16.66 (12)	−12.62 (10)	−15.16 (16)	−25.79 (10)	−17.82 (12)
Pt—As1—C111—C112	−152.5 (3)	−163.49 (20)	−164.41 (38)	−143.2 (3)	−142.0 (3)
Pt—As1—C111—C116	29.3 (3)	14.98 (24)	13.4 (4)	36.7 (3)	38.4 (3)
Pt—As1—C121—C122	54.5 (3)	46.03 (25)	43.6 (4)	54.2 (3)	43.5 (3)
Pt—As1—C121—C126	−124.1 (3)	−134.62 (22)	−137.0 (4)	−125.8 (3)	−132.1 (3)
Pt—As1—C131—C132	−115.0 (3)	−116.16 (25)	−114.3 (4)	−121.7 (3)	−113.7 (3)
Pt—As1—C131—C136	65.6 (3)	63.24 (26)	67.9 (4)	58.5 (3)	64.0 (3)

without any solvent molecule (1) gives the least efficient packing.

The van der Waals radii were used to calculate the free space in the structures (Spek, 1990). There is 20 Å^3 free space per Pt complex for (1), divided into two cavities of 10 Å^3 each, thus resulting in 2.4% free space per molecular unit. Structure (2) shows no detectable free space in the unit cell. In (3) a single cavity of 15 Å^3 is available per solvated Pt complex resulting in 1.6% free space per molecular unit. Compound (4) shows a single cavity of 24 Å^3 for each solvated Pt complex, resulting in 2.8% free space per molecular unit. All these fractions of free space found for the different complexes are too small for any additional solvent molecules to fit in. This shows that (2) fills the space in the unit cell most efficiently, *i.e.* there was no detectable free space found in the unit cell. Complex (3), which was earlier stated to have the most efficient packing (smallest volume per Pt complex), also fills the unit cell quite efficiently with only 1.6% free space.

By comparing all four structures with each other it was shown that all the phenyl rings are orientated in the same way around the platinum, *i.e.* all the Cl—Pt—As—C torsion angles are approximately the same in all four complexes (see Table 2). This is a very interesting observation due to the fact that the compounds do not crystallize similarly. This is being further investigated with molecular modelling to see if there are contributing electronic effects favouring this conformation. The torsion angles in the recently determined structure of *trans*-[PtCl$_2$(PPh$_3$)$_2$] were also found to be almost identical to those in the title complex (Johansson & Otto, 2000).

The Pt—Cl bonds are in the range 2.2839 (9)–2.3086 (17) Å and the Pt—As bonds are in the range 2.3923 (4)–2.4104 (4) Å. The Pt—Cl bond in (4) is smaller than the rest of

the Pt—Cl distances, and the Pt—As bond in (2) is smaller than the other Pt—As distances (see Table 2). The Cl—Pt—As angles are close to 90° in (1) and (3), ranging from 88.31 (5) to 91.69 (5)°, while those in (2) and (4) deviate more, ranging from 86.62 (2) to 93.20 (2)°. The As—Pt—As and Cl—Pt—Cl angles in (4) are 176.692 (11) and 178.79 (3)°, respectively, while all others have As—Pt—As and Cl—Pt—Cl angles of 180° due to symmetry requirements. In complexes (1), (2) and (3), and in ligand 4b, two of the Pt—As—C angles are similar and range from 111.53 (9) to 113.66 (9)°, while the third angle differs from the other two and is in the range 117.53 (9)–119.83 (13)°. The largest angle represents the phenyl ring lying almost in the coordination plane, *i.e.* with the smallest Cl—Pt—As—C torsion angle ranging from −12.62 (10) to −17.82 (12)°. For the other As ligand (4a) in compound (4) the Pt—As—C angles are in the range 110.11 (10)–121.26 (9)°. The smallest angle represents the Cl—Pt—As—C torsion angle closest to 90°, *i.e.* almost perpendicular to the coordination plane, minimizing steric interaction. Both the other two torsion angles are close to 0 and 180°, −25.79 (10) and −148.69 (10)°, respectively. From this it is apparent that two of the phenyl rings in (4a) experience steric interaction with a chloride, while the interaction is limited to only one phenyl ring for the other cases.

The closest contacts in the octahedral positions of the Pt atoms are in all cases to the H116 atom (intramolecular) with distances of 3.24, 3.13, 3.07 and 3.23 Å for compounds (1), (2), (3) and (4), respectively. The closest contact to the other octahedral position in (4) (not symmetry related) is also intramolecular (H212) at a distance of 3.38 Å. This longer contact distance in (4) is due to the benzene solvent molecule forcing the phenyl ring away.

The Pt—As bond distances are shown to be slightly longer than those found in most other Pt—As compounds, as indicated in Table 3. On comparing the title compounds with related *trans* bis-AsR_3 structures it can be seen that by changing Pt^{II} to Pd^{II} in a Cl/Cl system the Pt—Cl bonds tend to be slightly longer and the Pt—As bond slightly shorter compared with the analogous Pd complexes. Replacing As for P in a Pt^{II} complex with Cl/Cl and I/I coordination modes seems to have no effect on the bond distance of the chlorides, while the Pt—I bond is slightly lengthened for the As complex compared with the P analogue. An increase in the average Pt—L bond lengths (Table 3) for Pt—P [2.318 (2) Å], Pt—As [2.404 (2) Å] and Pt—Sb [2.552 (1) Å] follows the variation in the radius of P (1.10 Å), As (1.21 Å) and Sb (1.41 Å) (Sheldrick, 1997).

3.2. RMS calculations

RMS calculations provide a good estimate as to which structures are most similar (Sheldrick, 1997). It is interesting to note that (3), which displays the best packing efficiency, is involved in both the smallest [0.068 Å *versus* compound (2), Fig. 3*a*)] and the largest [0.268 Å *versus* compound (4), Fig. 3*b*] RMS value. The relative RMS deviation between (2) and (4)

(*a*)

(*b*)
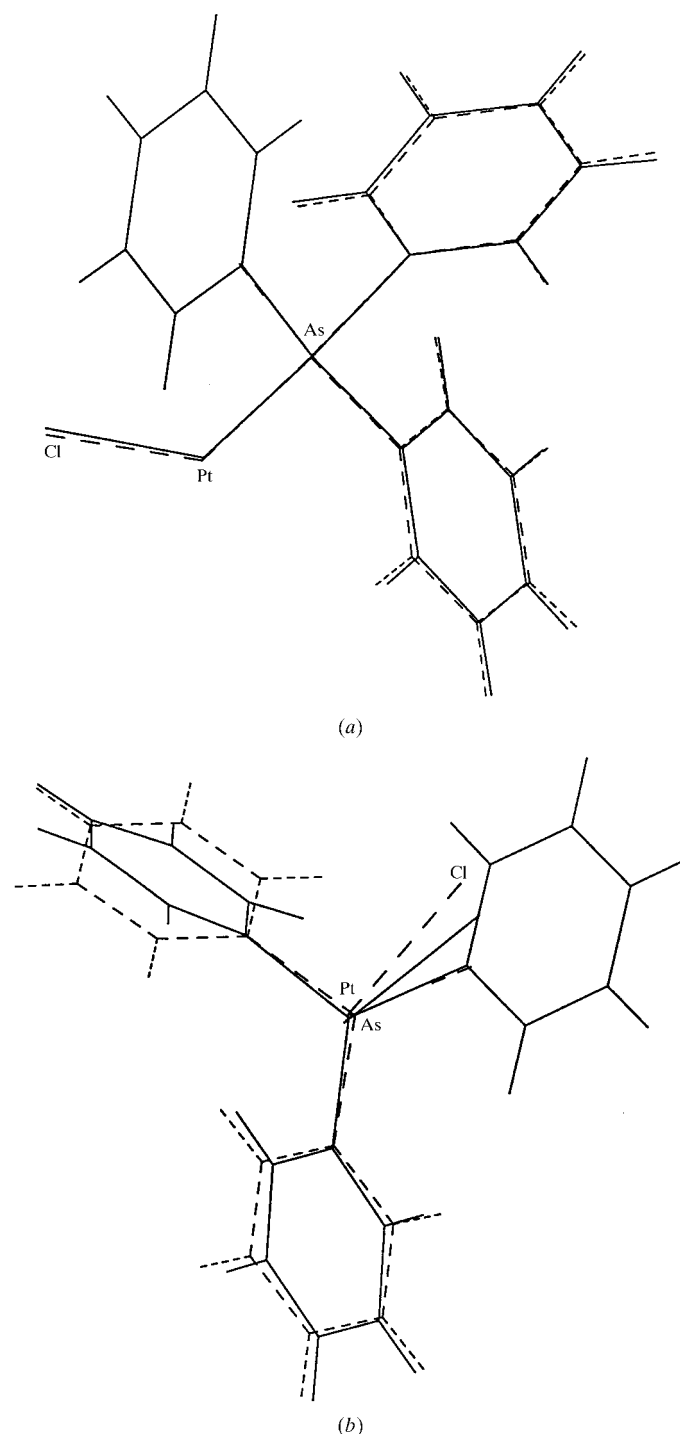
Figure 3
RMS plots to compare structural parameters between (*a*) (2) and (3), and (*b*) (3) and (4).

Table 3
Comparison of bond distances in *trans*-[$M(X)(Y)(L)_2$] complexes (M = Pt or Pd; X, Y = Cl, I or Me; L = P, As or Sb ligands).

Complex	$M-L$ (Å)	$M-Y$ (Å)	Reference
trans-[PtCl$_2$(PPh$_3$)$_2$]	2.3164 (11)	2.2997 (11)	(1)
trans-[PtCl$_2$(AsPh$_3$)$_2$]	2.4104 (4)	2.3003 (11)	(2)
trans-[PdCl$_2$(AsPh$_3$)$_2$]	2.423	2.284	(3)
trans-[PtMeCl(AsPh$_3$)$_2$]	2.3821 (9)	2.410 (2)	(4)
trans-[PtMeCl{As(*p*-Tol)$_3$}$_2$]	2.3879 (10)	2.397 (3)	(5)
trans-[PtI$_2$(PPh$_3$)$_2$]	2.318 (2)	2.603 (1)	(6)
trans-[PtI$_2$(AsPh$_3$)$_2$]	2.404 (2)	2.631 (2)	(7)
trans-[PtI$_2$(SbPh$_3$)$_2$]	2.552 (1)	2.602 (1)	(8)

(1) Johansson & Otto (2000); (2) this study; (3) Malinovskii *et al.* (1979) (s.u.'s not reported); (4) Roodt *et al.* (1995); (5) Otto & Roodt (1996); (6) Boag *et al.*, (1991); (7) Otto & Roodt (1997); (8) Wendt *et al.* (1998).

Table 4
Most disagreeable δm_i values for corresponding interatomic distances for the complexes compared in Figs. 4(*a*) and 4(*c*).

Fig. 4(*a*) [(2) *versus* (3)]			Fig. 4(*c*) [(3) *versus* (4)]		
δm_i	Distance	Order†	δm_i	Distance	Order†
20.11	Pt—As	First	26.74	Pt—C122	Third
12.04	Cl—As	Second	20.52	Cl—As	Second
8.43	Pt—C121	Second	20.44	Pt—C112	Third
5.80	Pt—C122	Third	11.99	Pt—C132	Third
4.92	Pt—C131	Second	7.76	C111—C121	Second
4.26	As—C116	Second	6.68	Pt—C121	Second
4.26	Pt—Cl	First	5.77	Pt—Cl	First
2.55	As—C131	First	5.76	Pt—C111	Second

† First-, second- and third-order number represents the closest distance between two atoms separated by one, two or three formal bonds.

also gives a high value of 0.266 Å. It should be noted that the large difference between (3) and (4*a*) [(2) and (4*a*)] is due to a twist of one of the phenyl rings, as well as the differences in the Cl—Pt—As—C torsion angles.

3.3. Half-normal probability plots

Half-normal probability plot analysis is used to (i) investigate the reliability of the s.u.'s and (ii) identify systematic geometrical differences in two molecules. Random errors of differences in interatomic distances are approximately normally distributed (Albertsson & Schultheiss, 1974). Observed values of δm_i calculated using equation (1) are plotted *versus* the values α_i expected for a half-normal distribution of errors (*International Tables for X-ray Crystallography*, 1974)

$$\delta m_i = \left| d(1)_i - d(2)_i \right| / [\sigma^2 d(1)_i + \sigma^2 d(2)_i]^{1/2}. \qquad (1)$$

The quantities $d(1)_i$ and $d(2)_i$ are interatomic distances for two different structures (1) and (2) with s.u.'s $\sigma d(1)_i$ and $\sigma d(2)_i$, respectively. Two kinds of comparisons are made, the first using dependent distances (representing atoms separated by one, two or three formal bonds) and the second using independent distances. For 21 non-H atoms (half the complex), 57 independent interatomic distances ($3n - 6$) completely describe the complex. To ensure a non-biased comparison only

57 dependent distances were used in the calculations. The dependent distances are used to identify distances that are significantly different for the compared molecules (Figs. 4a and 4c). From the graph obtained by using independent distances, a slope and an intercept are obtained (Figs. 4b and 4d). A linear plot with a slope of unity and a zero intercept indicates a correct match between the compared sets of distances and correctly estimated s.u.'s. If the slope is larger (or smaller) than unity the s.u.'s are underestimated (or overestimated). A non-linear plot, or a linear plot with a non-zero intercept, on the other hand, indicates systematic differences, which may be caused by geometrical differences in the compounds compared or by systematic errors in the measurement procedure.

Figs. 4(a) and 4(b) show half-normal probability plots for complex (2) compared with complex (3) (representing the best RMS fit) and Figs. 4(c) and 4(d) show comparisons of complexes (3) and (4) (representing the worst RMS fit). The largest systematic differences for Figs. 4(a) and 4(c) are shown in Table 4. Fig. 4(b) shows linearity up to $\alpha_i = 1.06$ ($R = 0.98$), with a slope of 2.30 ± 0.11 and intercept 0.11 ± 0.07 (95% confidence interval), while Fig. 4(d) shows linearity up to $\alpha_i = 1.51$ ($R = 0.98$), with a slope of 4.78 ± 0.21 and intercept 0.69 ± 0.16 (95% confidence interval). The intercept indicates that there are systematic differences between both (2)–(3) and (3)–(4). On the assumption that the s.u.'s are underestimated to the same extent in all the structures (similar weighting schemes have been used), the relative underestimations are in the range 2.3–4.8. It is clear from Table 4 and from the

intercepts in Figs. 4(b) and 4(d) that the systematic differences between (3) and (4) are larger than those between (2) and (3).

4. Conclusions

For all the compared structures [(2), (3) and (4); Fig. 4] the s.u.'s are shown (by the slope) to be underestimated and the intercepts are indicative of small systematic differences between the structures. Both RMS (Fig. 3) and the intercepts in the plots indicate that the structures (2) and (3) are the most similar. Systematic differences are mainly in the second- and third-order distances, except for the Pt—As and Pt—Cl bond distances (first order), which show significant differences as well (Table 4). Even if neither the Pt—Cl nor the Pt—As distances are normally distributed, the average values and the dispersions give information of the softness of these bonds and thus the expected maximum variation due to all factors involved. The average distances are $\overline{d}_{\text{Pt--Cl}} = 2.298\,(9)$ and $\overline{d}_{\text{Pt--As}} = 2.405\,(7)$ Å, with the error calculated from $s_{\text{tot}} = [\Sigma(d - \overline{d})^2/(n-1)]^{1/2}$, corresponding to 2.298 (25) and 2.405 (19) Å for a 95% confidence interval. It is of interest to estimate the contribution of packing forces to the total dispersion, s_{tot}. In general the variance s_{tot}^2 may be considered composed of $s_{\text{pre}}^2 + s_{\text{acc}}^2 + s_{\text{intra}}^2 + s_{\text{env}}^2$, where s_{pre} refers to precision (s.u.'s), s_{acc} to systematic errors, s_{intra} to intermolecular factors and s_{env} to packing effects. In this case s_{intra} is zero (exactly the same complex in all cases), s_{acc} is small (according to normal probability plots), and the s.u.'s are underestimated by a factor of roughly 3–4 (according to normal probability plots). By taking these factors into account, the parameter s_{env} is 0.008 and 0.007 Å for the Pt—Cl and Pt—As bonds, respectively. Thus, the whole dispersion essentially originates from the different packing arrangements and both Pt—Cl and Pt—As distances may vary as much as 0.020–0.025 Å in different compounds due to packing forces. This may be compared with the values 0.01–0.02 for a large amount of M–L data reported by Martín & Orpen (1996). The closest contacts between the metal complexes and the solvent molecules are always Cl···H interactions, which are 2.74, 3.05 and 3.23 Å in (2), (3) and (4), respectively. This indicates that electronic interactions are at most very moderate, although the chlorinated solvent H atoms are directed towards the Cl atoms, and the observed effects may thus be more due to steric strain. Similar Cl—Pt—As—C torsion angles were
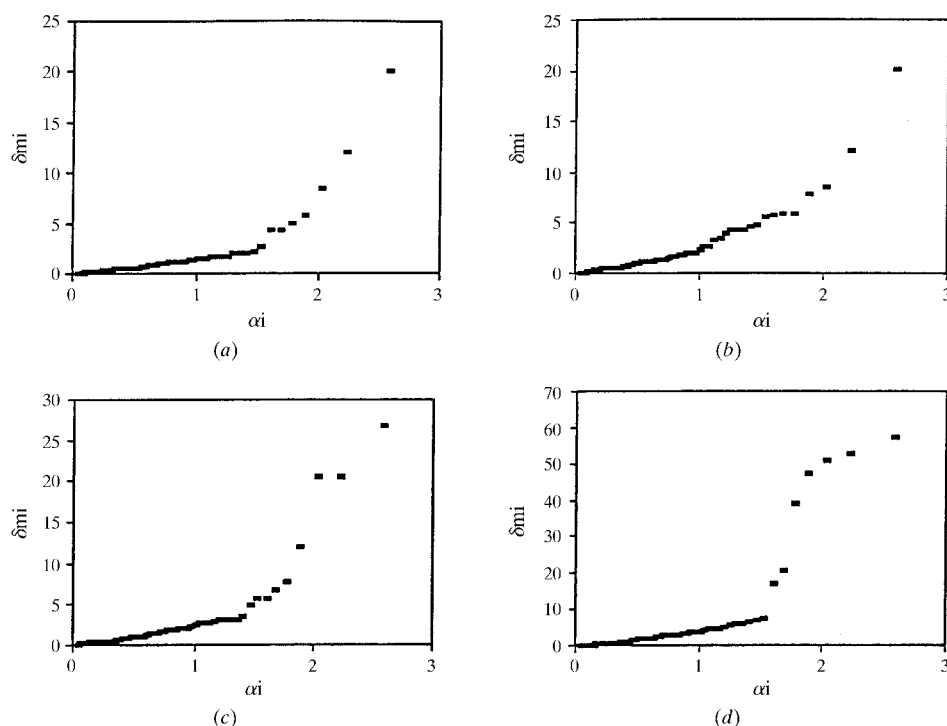
Figure 4
Half-normal probability plots. (a) (2) versus (3), based on 57 dependent distances; (b) (2) versus (3), based on 57 independent distances; (c) (3) versus (4), based on 57 dependent distances; (d) (3) versus (4), based on 57 independent distances.

observed in all the structures, except for ligand (4*a*), which differs by about 10° from the others.

References

Abrahams, S. C. & Keve, E. T. (1971). *Acta Cryst.* A**27**, 157–165.

Albertsson, J. & Schultheiss, P. M. (1974). *Acta Cryst.* A**30**, 854–855.

Bacon, G. E., Curry, N. A. & Wilson, S. A. (1964). *Proc. R. Soc. London Ser. A*, **274**, 98–110.

Belsky, V. K., Konovalov, V. E., Kukushkin, V. Y. & Moiseev, A. I. (1990). *Inorg. Chim. Acta*, **169**, 101–107.

Boag, N. M., Mohan Rao, K. & Terrill, N. J. (1991). *Acta Cryst.* C**47**, 1064–1065.

Boese, R., Blaeser, D. & Haumann, T. (1992). *Z. Kristallogr.* **198**, 311–312.

Brandenburg, K. (1997). *DIAMOND.*. Version 2.1. Crystal Impact, Bonn, Germany.

Collimati, I., Furlani, A. & Attioli, G. (1970). *J. Chem. Soc. (A)*, pp. 1694–1696.

Cox, E. G., Saenger, H. & Wardlaw, W. (1934). *J. Chem. Soc.* pp. 182–186.

De Camp, W. H. (1973). *Acta Cryst.* A**29**, 148–150.

Ericson, V., Lövqvist, K., Norén, B. & Oskarsson, Å. (1992). *Acta Chem. Scand.* **46**, 854–860.

Johansson, M. H. & Otto, S. (2000). *Acta Cryst.* C**56**, e12–e15.

Kapoor, P., Kukushkin, V. Y., Lövqvist, K. & Oskarsson, Å. (1996). *J. Organomet. Chem.* **517**, 71–79.

Kawaguchi, T., Tanaka, K., Takruchi, T. & Watanabe, T. (1973). *Bull. Chem. Soc. Jpn*, **46**, 62–66.

Kemp, G., Roodt, A. & Purcell, W. (1995). *Rhodium Express.* **12**, 21–26.

Kitaigorodsky, A. I. (1973). *Molecular Crystals and Molecules.* New York/London: Academic Press.

Lövqvist, K. (1996). Thesis. University of Lund, Sweden.

Malinovskii, S. T., Bourshteyn, I. F. & Malinovskii, T. I. (1979). *Izv. Akad. Nauk. Mold. SSR. Ser. Fiz.-Tek. Mater. Nauk.* pp. 45–48.

Martín, A. & Orpen, A. G. (1996). *J. Am. Chem. Soc.* **118**, 1464–1470.

Microsoft (1997). *Program for Spreadsheets and Graphics.* Microsoft Inc., USA.

Otto, S. & Roodt, A. (1996). *Acta Cryst.* C**52**, 1636–1638.

Otto, S. & Roodt, A. (1997). *Acta Cryst.* C**53**, 280–282.

Roodt, A., Otto, S. & Leipoldt, J. G. (1995). *Acta Cryst.* C**51**, 1105–1106.

Sheldrick, G. M. (1990). *SHELXS*86. University of Göttingen, Germany.

Sheldrick, G. M. (1996). *SADABS.* University of Göttingen, Germany.

Sheldrick, G. M. (1997*a*). *SHELXL*97. University of Göttingen, Germany.

Sheldrick, G. M. (1997*b*). *SHELXTL*97. University of Göttingen, Germany.

Siemens (1995). *SAINT.* Siemens Analytical X-ray Instruments Inc., Madison, Wisconsin, USA.

Siemens (1996). *SMART.* Siemens Analytical X-ray Instruments Inc., Madison, Wisconsin, USA.

Silver, L. & Rudman, R. (1972). *J. Chem. Phys.* **57**, 210–216.

Spek, A. L. (1990). *Acta Cryst.* A**46**, C-34.

Watkins, S. F. (1970). *J. Chem. Soc. A*, 168–172.

Wendt, O. F., Scodinu, A. & Elding, L. I. (1998). *Inorg. Chim. Acta*, **277**, 237–241.